The Plasma Dynamics of Hypersonic Spacecraft: Applications of Laboratory Simulations and Active In Situ Experiments

N. H. Stone
Space Science Laboratory
NASA Marshall Space Flight Center
Huntsville, Alabama 35812

and

Uri Samir
Space Physics Research Laboratory
University of Michigan
Ann Arbor, Michigan 48109

Abstract: Attempts to gain an understanding of spacecraft plasma dynamics via experimental investigation of the interaction between artificially synthesized, collisionless, flowing plasmas and laboratory test bodies date back to the early 1960's. In the past 25 years, a number of researchers have succeeded in simulating certain limited aspects of the complex spacecraft-space plasma interaction reasonably well. Theoretical treatments have also provided limited models of the phenomena. However, the available in situ data was fragmentary, incomplete, and unable to provide a good test for the results from ground based experiments and theory. Several active experiments were recently conducted from the space shuttle that specifically attempted to observe the Orbiter-ionospheric interaction. These experiments have contributed greatly to an appreciation for the complexity of spacecraft-space plasma interaction but, so far, have answered few questions. Therefore, even though the plasma dynamics of hypersonic spacecraft is fundamental to space technology, it remains largely an open issue. This paper provides a brief overview of the primary results from previous ground-based experimental investigations and the preliminary results of investigations conducted on the STS-3 and Spacelab 2 missions. In addition, several, as yet unexplained, aspects of the spacecraft-space plasma interaction are suggested for future research.

1. INTRODUCTION

Any object placed in space will be immersed in a macroscopically neutral conglomeration of positively and negatively charged particles, as well as neutral particles, generally called a plasma. The space plasma is, although very tenuous, an important component of the space environment--of critical importance to many geophysical and active plasma investigations as well as to the environmental dynamics of large space structures such as the space station. However, today after three decades of space flight, there still remain a number of open questions and unexplained effects that require the attention of future research efforts.

The physics of a body immersed in a quiescent, collisionless plasma is well understood: the body takes on an electric (floating) potential which

tends to balance the flux of charged particles to its surface so that no net electrical current flows. The plasma tends to shield itself from this potential by creating a region of unequal ion and electron number density surrounding the body, called the plasma sheath, in which the floating potential on the body is matched to the space potential of the plasma. However, when a relative motion exists between a body and its environmental space plasma, an interaction occurs which is far more complex than the simple quiescent case. A redistribution of surface charge occurs on the body and the zone of disturbance in the plasma is no longer radially symmetric, regardless of body geometry. When the relative motion between the body and plasma is mesosonic, as it is in the lower ionosphere, several characteristic processes have been found to occur: the plasma sheath on the frontal side of the body may be compressed to some extent by the directed motion of the ions; immediately behind the body, the more massive particles are swept out leaving a region essentially void of ions and neutrals; potential wells and oscillations may occur, ions are accelerated into the void region and ion beams and plasma waves propagate into, and away from, the wake. Although the electron mobility is sufficiently great to populate the void region from relative velocity considerations, a negative space charge potential is created by their presence which tends to impede their motion into the region. Hence, the void region that occurs in the wake near the body is highly depleted of all charged and neutral particles and forms the most intense feature of the body-plasma interaction.

The way in which the void region is repopulated may result from a variety of mechanisms including the focusing of ions by electric fields in the plasma sheath surrounding the front half of the body, ambipolar diffusion, thermal diffusion, the plasma expansion phenomena, and scattering by various plasma oscillations or instabilities. Other characteristics of hypersonic plamsa dynamics include the spatial extent of the interaction region, the rate at which the disturbances propagate outward downstream from the body, and effects that occur in the wake after the void region has been repopulated (Figure 1). For example, in cases where the electrostatic focusing in the plasma sheath dominates, some ions may be deflected onto the trailing surfaces of the body and a region of significant ion number density enhancement has been observed to occur downstream on the wake axis at the crossing point of the deflected ion trajectories.

The dominate characteristics of plasma flow interactions and the governing physical mechanisms depend on the various body and plasma parameters such as scale size, electron-to-ion temperature ratio, ion acoustic Mach number, and body potential--the effects of which are understood only over limited regions of parameter space. Moreover, the discussion, so far, has dealt only with simple conducting bodies and non-magnetized, collisionless plasmas. Clearly, other complicating factors exist, such as neutral gas emissions from the spacecraft, collisional effects, secondary electron emission, solar UV, chemical reactions, multiple ion species, and magnetic fields. Since the relative motion between the body and the plasma is supersonic with respect to certain ion plasma waves, a collisionless shock wave may be expected to occur under some circumstanes. It is further thought that secondary electron emission may lead to a non-monotonical matching in the plasma sheath of the floating potential on the body with the, generally more positive, space potential of the environmental plasma. Although it is recognized that these effects can occur in space, they have been beyond the scope of most experimental and theoretical studies, which usually treated only small scale,

conducting bodies of relatively simple geometry, in collisionless, unmagnetized plasmas of a single ionic species (for a review see Stone, 1981a).

Although it has long been recognized that the spacecraft-space plasma interaction occurs and can adversely affect spacecraft systems as well as scientific instrumentation (Stone et al., 1978), most space missions have involved single satellites which, a priori, could provide only very limited information. Therefore, with the possible exception of the Gemini-Agena 10 and 11 missions, no deliberate and systematic attempt has been made to study the problem in space prior to the advent of the space shuttle. As a result, the in situ data available from the 60's and 70's are incomplete in spatial coverage and fragmentary in the sense that seldom were all the necessary measurements made (for a review see Samir, 1973).

In the absence of definitive in situ measurements, a large number of theoretical and ground-based experimental studies were made during this period. Although much valuable information has been gained from these efforts, both approaches have limitatins and the field of spacecraft plasma dynamics, or ionospheric aerodynamics, is far from being well understood. The results from recent space shuttle missions have answered few questions to date, but rather, have contributed to a greater appreciation for the complexity of spacecraft-space plasma interactions.

The intent of this paper is to touch briefly on the major contributions of previous experimental investigations, provide examples of the corroboration of the interpretation of in situ measurements by the understanding gained from groundbased investigations, and discuss the main features of the STS-3 and Spacelab 2 space shuttle investigations.

2. MATHEMATICAL FORMULATION

In the kinetic, formulation of plasma flow problems, since a plasma consists of a number of different types of particles, including electrons, ions, and neutral molecules, a complete statistical description of the state of the plasma requires a separate function, $f_\alpha(\vec{x},\vec{v},t)$, to describe the distribution of each constituent in six dimensional phase space at some given time. Each of these distribution functions is the solution of a Boltzmann equation of the form:

$$\frac{\partial f_\alpha}{\partial t} + \vec{v}\,\frac{\partial f_\alpha}{\partial \vec{x}} + q_\alpha[\vec{E} + \vec{v} \times \vec{B}/C]\quad \frac{\partial f_\alpha}{\partial \vec{v}} = \left(\frac{\partial f_\alpha}{\partial t}\right)_c , \qquad (1)$$

which describes the rate of change of the distribution of the α-constituent, f_α, in space and time. Alternatively, this equation can be viewed as a statement of the conservation of particles existing in an elemental volume of phase space, $d^3x\ d^3v$.

The term on the right-hand side of the equation, $(\partial f_\alpha/\partial t)$, accounts for short range, discrete collisions, which may be electrostatic in nature (between two charged particles) or "hard sphere" type collisions.

The Lorentz force, $q_\alpha [\vec{E} + \vec{v} \times \vec{B}/C]$, results from the self-consistent electrostatic and magnetic fields which account for "distant collisions" of particles with long range forces. A collective behavior then results from Coulomb interactions between groups of charged particles.

The Lorentz force is made self-consistent by requiring it to satisfy the Maxwell equations:

$$\nabla \times \vec{B} = \frac{1}{c} \frac{\partial \vec{E}}{\partial t} + 4\pi \vec{J} \tag{2}$$

$$\nabla \times \vec{E} = - \frac{1}{c} \frac{\partial \vec{B}}{\partial t} , \tag{3}$$

and the Poisson equation:

$$\nabla \cdot \vec{E} = 4\pi \rho_c , \tag{4}$$

where $\vec{J}$ is the total current flow and ρ_c is the net charge density.

The current and net charge density, in turn, depend on the distribution functions of the plasma constituents (solutions of the Boltzmann equations) through the relations

$$\vec{J} = \vec{J}_{ext} + \sum_\alpha q_\alpha \int \vec{v} f_\alpha (\vec{x},\vec{v},t) \, d^3v \tag{5}$$

and

$$\rho_c = \sum_\alpha q_\alpha \int f_\alpha (\vec{x},\vec{v},t) \, d^3v . \tag{6}$$

Equations (1) through (4), subject to the definitions (5) and (6), form the governing equations for plasma flow interactions. This set of partial differential equations is coupled and nonlinear. Therefore, a number of simplifying assumptions and approximations are generally made in kinetic treatments to obtain a tractable problem. In effect, most experimental models have made many of the same simplifications.

First, it is generally assumed that the flow interaction exists in a steady state. While this obviously has a great impact on the complexity of the equations, its physical justification is questionable. There is no description of time dependent effects. There exist, however, experimental evidence that suggests the presence of wave particle interactions in the wake region.

A second widely used assumption is that the magnetic field can be omitted, which reduces the Lorentz force to $q_\alpha \vec{E}$. There is some experimental justification for this assumption under certain conditions. This assumption coupled with the previous assumption that $\partial/\partial t = 0$ eliminates Maxwell equations (2) and (3), leaving only the Poisson equation (4) that the electric field must satisfy. From equation (5), we see that the only currents possible are those resulting from external forces, which are generally omitted.

The third major assumption is that the plasma is "collisionless." This means that, although long range, collective interactions will occur and must be considered, the short range, discrete collisions occur so infrequently as to have a negligible effect. Since the discrete collisions are negligible, we set $(\partial f_\alpha/\partial t) = 0$ and equation (1) becomes homogeneous (the Vlasov equation). Moreover, since neutral particles interact through discrete collisions (which are assumed to be negligible) they can be completely neglected. We, therefore, only require time independent collisions Boltzmann (or Vlasov) equations for ions and electrons; i.e..,

$$\vec{v}\cdot\frac{\partial d_{i,e}}{\partial \vec{x}} + q_{i,e}\vec{E}\cdot\frac{\partial f_{i,e}}{\partial \vec{v}} = 0 \ . \tag{7}$$

A fifth general assumption is that the flow is mesothermal; i.e., $\bar{c}_i << V_o << \bar{c}_e$, where $\bar{c}_{i,e}$ is the mean thermal speed of ions or electrons and V_o is the orbital speed. Since the mean thermal velocity of the ions is negligibly small compared to the relative motion between the body and the plasma, the ions can be assumed to behave as a monoenergetic stream (no thermal motion). The electrons, on the other hand, have a mean thermal speed much greater than the orbital speed and maintain a Maxwellian distribution in the presence of a repulsive body potential.

The boundary condition generally assumed at the body states that the body is an equipotential surface and that all incident charged particles are neutralized; i.e., no charged particles are reflected from the surface. The potential is assumed to go to zero (plasma potential) infinitely far from the body.

3. SCALING LAWS

The dimensionless parameters that must be invariant in order to obtain strict similitude between two flow interactions of different scale sizes can be derived formally from the governing equations (1-4). We also apply here the general assumptions discussed above. Making the variable substitutions:

$$x = R_o X \qquad t = \mathfrak{T}/\omega \qquad v = V_o u \qquad f_i = n_o F$$

$$\phi = P\Phi \qquad q_i = eZ \qquad m_i = m_p M \qquad n_{i,e} = n_o N_{i,e},$$

$$\hat{\nabla} = \nabla/R_o \ ,$$

the governing equations take the dimensionless form:

$$N_e = \exp\left[\Phi\left(\frac{eP}{kT_e}\right)\right] \tag{7}$$

$$\left(\frac{\omega R_o}{V_o}\right)\frac{\partial F}{\partial t} + \vec{u}\cdot\nabla F_i - \left(\frac{ZeP}{m_p M V_o^2}\right)\nabla\Phi\cdot\frac{\partial F_i}{\partial \vec{u}} = 0 \tag{8}$$

and

$$\nabla^2\Phi = -\left(\frac{4\pi e n_o R_o^2}{P}\right)\left[ZN_i - N_e\right] . \tag{9}$$

The equations (7-9) will remain invariant if we require $P = kT_e/e$ and the following parameter groups to remain constant:

$$Z \equiv \text{number of charges per ion} \tag{10}$$

$$\left[\frac{e\phi}{kT_e}\right] = \Phi \tag{11}$$

$$\left[\frac{\omega}{V_o/R_o}\right] \tag{12}$$

$$\left[\frac{ZeP}{m_p M V_o^2}\right] = \frac{ZkT_e}{m_i V_o^2} = \left(\frac{Z}{2}\right) S^{-2} \tag{13}$$

$$\left[\frac{4\pi e n_o R_o^2}{P}\right] = \left(\frac{4\pi n_o e^2}{kTe}\right) R_o^2 = \left(\frac{R_o}{\lambda_D}\right)^2 = R_d^2 . \tag{14}$$

Hence, the dimensinoless parameters, Debye ratio, R_d, Ion acoustic Mach number, S, and normalized electric potential, Φ, arise naturally from the governing equations. The necessity of scaling all three parameter groups was shown experimentally by Skvortsov and Nosachev (1968a) in that measurements taken for constant values of R_d, S, and Φ_b, obtained at different values of T_e, show little variation while a significant variation appears in some cases when only the ratios R_d and ϕ_b/S^2 were preserved.

In principle, it should be possible to obtain any arbitrary combination of the dimensionless scaling parameters R_d, S, and Φ_b by appriopriate choices of the physical variables n_o, T_e, V_o, and R_o. Unfortunately, this is not the case since, in practice, several of these variables are subject to experimental limitations. The test body size must be smaller than the plasma stream, therefore, making the plasma source radius an upper bound for the body radius, R_o. Further, due to the nature of ion accelerators, it is difficult to obtain high number densities in low energy streams.

The above limits impose no constraint on Φ_b ($\sim\phi_b/T_e$) since, in the laboratory, ϕ_b is independent of all other variables and can be adjusted to any desired value by an external voltage source. Similarly, R_d ($\sim n_o R_o^2/T_e$) can be made arbitrarily small and S ($\sim V_o^2/T_e$) arbitrarily large by making R_o small and V_o large, respectively. However, R_d cannot be made arbitrarily large while making S small. Since R_o must be less than the beam radius, any further increase of R_d must be accomplished by increasing n_o and/or decreasing T_e. However, this is inconsistent with small S which requires small V_o (and

therefore small n_o) and/or large T_e. The conditions of large R_d and small S are therefore mutually exclusive in the laboratory and can only be approached within certain practical limits.

As a result of the practical constraints on R_d and S, it will be possible to correctly scale very few of the wide range of conditions possible for orbiting satellites or diagnostic instruments in the ionospheric plasma according to the strict Vlasov scaling laws developed above. In recent years, however, a concept known as qualitative scaling has evolved which allows a considerable relaxation of the rigid Vlasov laws (Fälthammar, 1974). Under qualitative scaling, parameters much greater (or smaller) than unity are required to remain so but are not required to maintain the same order of magnitude. Only parameters which are of order unity must be scaled closely; i.e.,

	$>>1$		$>>1$
P_{space}	$<<1$	P_{LA_B}	$<<1$
	~ 1		$\simeq P_{space}$

Qualitative scaling has greatly extended the applicability of groundbased experiments to natural in situ phenomena. Further, it allows additional aspects of the problem, such as magnetic and temporal effects, to be included.

4. AN OVERVIEW OF GROUNDBASED LABORATORY INVESTIGATIONS

Most laboratory research has centered around the near to mid-wake regions of small bodies ($R_d \sim 1$ to 10) in nonmagnetized plasma streams. The primary results for this case will be discussed below. For a discussion of the upstream and far-wake disturbance, the reader is referred to the work of Fournier (1971), Hester and Sonin (1970a,b), and Woodroffe and Sonin (1974). The dynamics of magnetized plasmas has been studied by Astrelin et al. (1973) and Bogasheohento et al. (1971).

1. Simulation of the Spacecraft-Ionospheric Interaction

(1) The Disturbance Envelope

The envelope of the zone of disturbance, defined by the boundary between freestream conditions ($J_i/J_{io} = 1$) and disturbed flow ($J_i/J_{io} \neq 1$), depends on two factors: the initial width of the disturbance at the largest cross section of the test body, and the rate at which the disturbance propagates away from the Z-axis as it moves downstream. The initial radial extent of the disturbance, defined by the sum of the test body radius and the sheath thickness, was found to increase in proportion to the ion acoustic Mach number and the negative body potential as $|-\phi_b|^{1/2}S$ (Figure 2). It can also be expected to increase with the Debye length. The propagation of the disturbance boundary away from the wake axis was found to define a Mach cone (Skrortsov and Nosachev, 1968b, and Stone et al., 1978) based on the ion acoustic Mach number, S. This result is in agreement with several theoretical treatments, including those of Rand (1960a,b) and Maslennikov and Sigov (1965, 1967, 1969) which predict a Mach cone structure for bodies with a small

potential Φ_b. The rarefaction wave, which is the most spatially extensive characteristic of the disturbance, was found to decrease the ambient ion current density by as much as a factor of three at distances as great as $2(S \cdot R_o)$ downstream (Stone et al., 1978).

The above conclusions are based on the parameter range R_d = 4 to 6, S ≃ 11, and Φ_b = -3.8 to -47. Measurements by Hester and Sonin (1969a,b; 1970) show the existence of pseudowaves (streams of ions deflected across the wake axis by the sheath fields) for $\Phi_b >> S$. These ion streams may overrun the rarefaction wave, under certain conditions, and extend the zone of disturbance beyond the mach cone.

(2) Ion Trajectory Focusing by the Plasma Sheath

The focusing of ion streams onto the wake axis by the electric field existing in the plasma sheath surrounding a test body was inferred in early studies by the presence of diverging wave-like structures in the far-wake region (Hester and Sonin, 1970a,b and Stone et al., 1972, 1974). More recent, direct vector measurements of deflected ion streams show their angle of attack to be proportional to Φ_b in the near wake for small scale bodies (Stone, 1981b).

The vector ion flow measurements also revealed a "bunching" of the ion trajectories at the radial boundaries of the ion void region, which can be seen in the current density profiles of Figure 3. This effect was not discussed in early theoretical or experimental studies (Stone, 1981a), although it is apparent in the theoretical results calculated by Maslennikov and Sigov (1969).

The present experimental data are not sufficient to reveal the physical mechanism which produces the observed ion trajectory "bunching" in the near wake. Neither do the calculations of Maslennikov and Sigov allow an explanation, and the the effect does not even occur in other theoretical treatments such as the one by Call (1969), which predicts a "fanning out" of the deflected ion trajectories. The near-wake ion trajectory grouping may be produced either by a collective effect on the ions (possibly a result of instabilities set up by the large density gradient at the void boundary) or by a nonmonotonic potential gradient in the plasma sheath.

(3) The Axial Ion Peak

Early investigations by Hall, Kemp, and Sellen (1964) clearly show the ion void in the near-wake region and an axial ion peak for a spherical test body. The ion current density was measured at a number of stations across the wake for a wide range of body potentials, revealing a distinct dependence of the axial ion peak on Φ_b. More detailed measurements of the ion peak, including both transverse and axial profiles for a variety of potentials, were published a year later by Clayden and Hurdle (1966). These measurements, in addition to showing a dependence on Φ_b, show the axial ion peak to rise rapidly behind the body and trail off slowly, extending more than 20 R_o downstream. Similar results were found for a sphere and a conical body oriented with its apex into the flow.

Converging ion streams at the boundaries of the wake void region were found to create the initial ion peak on the wake axis (Stone, 1981c). The position of this peak was found to depend on S, R_d, and Φ_b as shown in Figure 4. This result agrees closely in its S and Φ_b dependences with the theoretical predictions by Martin (1974). A second peak may also created on the wake axis further downstream. The two types of axial ion peaks are normally superpositioned for small Φ_b and cannot be distinguished from each other. However, they tend to separate at highly negative Φ_b values, indicating that a second casual mechanisms with a different dependence on Φ_b may be involved--possibly the collisionless plasma expansion phenomenon.

The height and width of the axial ion peak at the location of its maximum amplitude were also investigated (Stone, 1981c). The maximum peak height for spherical test bodies was found to be proportional to $[S/|\Phi_b|]^{1/2}$ as shown in Figure 5. The peak width (normalized by the test body radius, R_o) was found to depend only on $|\Phi_b|^{-1/2}$ (Figure 6). This dependence is taken to represent a balance between the momentum the particles obtain due to deflection toward the Z-axis, produced by ϕ_b, and the magnitude of the space charge potential barrier on the Z-axis, which is proportional to kT_e. (Note that $\Phi_b = e\phi_b/kT_e$.)

It was also found that the nature of the axial ion peak depends strongly on the cross-sectional geometry of the test body. This can be explained simply by the behavior of the plasma sheath, which is directly pro portional to $|\Phi_b|^{1/2}/S)$. For small Φ_b and large R_d, the sheath is thin compared to the test body dimensions and conforms closely to its geometry. For a test body having a square cross section, the ion streams were found to be deflected onto lines that are orthogonal at the Z-axis and approximately a body diameter in length. This produces a wider peak of lower amplitude. As Φ_b becomes large or R_d becomes small, the sheath becomes relatively thick, expands away from the body and acquires a more spherical shape. Hence, the ions are deflected more toward a point on the Z-axis and the axial ion peak structure will take on a behavior more characteristic of spherical test bodies.

The effects of test body geometry were studied in a preliminary manner and indicate that the wake of a geometrically complex body may be explained in terms of a linear superposition of the wakes of its different, simple, geometric constituents (Stone, 1981a).

(4) Deflection of Ion Trajectories in the Mid-Wake Region

The deflection of ion trajectories in the mid-wake region was first predicted theoretially by Maslennikov and Sigov (1969) and later by Call (1969) although not to the same degree due to the limitations imposed by his flux tube technique. In both cases, the ion trajectories were found to be deflected away from the Z-axis by the positive space charge potential associated wih the mid-wake axial ion peak. this effect was inferred by Hester and Sonin (1970) from the nature of the diverging wave-like structure they observed in the far wake. More recent vector ion flow measurements show that ion streams exist within the plasma wake with angles of inclination to

the Z-axis smaller than the geometric angle defined by the radial extent of the test body (Stone, 1981a). Since ion streams obviously cannot pass through the test body and do not originate on its rear surface, this is taken as clear evidence that the streams, initially deflected toward the Z-axis, subsequently underwent an additional deflection away from the Z-axis somewhere downstream--presumably at the location of the axial ion peak.

(5) Effects of Ion Thermal Motion

An extensive experimental study of this effect was carried out by Fournier and Pigache (1975) and it has been studied theoretically by Taylor (1967), Gurevich, et al. (1969), and Fournier (1971). While it is clear that the general effect of ion thermal motion is to diffuse the detailed wake structure discussed above, the more quantitative question as to how effective this diffusion process is, or at what T_e/T_i value the structure vanishes, has not been satisfactorily resolved. The calculations by Fournier for a long cylindrical body show that a nonmonotonic n_i distribution continued to exist in the wake for $\Phi_b \leq -2.75$ when $T_e/T_i = 2$ and for $\Phi_b \leq -6$ when $T_e/T_i = 1$. Moreover, the experimental observations by Fournier and Pigache (1975) show the peak structure to completely vanish only for small Φ_b and $T_e/T_i < 1$ (Figure 7). It appears that the opposing effects of Φ_b and T_e/T_i are such that for small Φ_b the axial ion peak vanishes for $T_e/T_i \simeq 1$, but can be recreated by a sufficiently negative value of Φ_b. We may, therefore, conclude that in the ionosphere, where for $T_e/T_i \simeq 2$ and $\Phi_b \simeq -5$, the axial ion peak can be expected to occur to some extent. This conclusion is supported by the clear presence of an axial electron peak (which in laboratory studies is smaller than the ion peak) in the wakes of the Ariel I satellite and its spherical ion probe (Henderson and Samir, 1967).

(6) Effects of Large R_d Values

Laboratory and theoretical studies have been limited to R_d values less than 50, which do not approach the R_d range of large space platforms. However, several parametric trends have been established that may be cautiously extrapolated to describe large bodies in Earth orbit.

It was pointed out above that the amplitude of the axial ion peak significantly depends only on S and Φ_b and, further, that the peak width (normalized by body radius) depends only on Φ_b. If these observations, made over a relatively small range of R_d, can be extrapolated to large R_d values, then, on this basis, the axial ion peak would be expected to maintain an approximately constant width (relative to the body radius) and amplitude as R_d increased arbitrarily.

This conclusion is incomplete, however, without considering the effects of ion thermal motion. The tendency of random motion to spread out and diminish the wake structure can be expected to increase with the distance traveled by the ions, and hence with R_d. Therefore, it becomes doubtful that the detailed wake structure discussed above would be observed for very large bodies in the ionosphere at floating potential. However, if the body potential became elevated (such as may occur in the case of the Space Shuttle orbiter when charged particle accelerators are fired or as the result of $(\vec{v} \times \vec{B}) \cdot \vec{L}$ potentials on very large structures such as the Space Station) the wake structure may appear as a result of the opposing effect of Φ_b shown by Fournier.

(8) Magnetic Field Effect

The effects of the geomagnetic field on spacecraft plasma dynamics have been included in only a few laboratory investigations; e.g., Bogashchento et al. (1971) and Astrelin et al. (1973). In particular, it was found that the net result of a parallel magnetic field is the generation of standing axial ion current density oscillations along the wake axis with a period proportional to $(Z\omega_{ci}/2\pi V_o)$. Evaluating these results for typical ionospheric conditions shows that such oscillations would be very small in amplitude and that the period would extend far beyond the mid-wake zone. Therefore, it is concluded that the omission of the geomagnetic field in studies of the near- and mid-wake regions of small to medium sized bodies is justifiable.

2. Process Simulation Experiments

As stated in section 3, process scaling involves the philosophy of qualitative scaling to study an individual physical process that may be one of many involved in a complete phenomonon. Activity in this area has picked up considerably in recent years. We will briefly discuss three examples: the investigation of collisionless plasma expansion across a strong density gradient, the possible coupling between widely separated current sources in the magnetized ionospheric plasma, and electron heating of the near wake.

(1) Expansion of a Collisionless Plasma:

The collisionless expansion of a large reservoir of plasma across a strong density gradient is greatly influenced by an electric field created at the expansion front by high speed electrons separating from the massive ion component. The ions are, in turn, accelerated to high velocities (several times the ion acoustic speed) by the field, which is maintained by a continual replenishment of fast electrons at the front from the plasma reservoir. A recent review of the phenomenon and its possible occurrence in space plasmas is given by Samir et al. (1983). A laboratory process simulation investigation of collisionless plasma expansion is in progress at MSFC (Wright et al., 1985; 1986, and several other institutions (Chan et al., 1984).

Figure 8 is a schematic of the basic process as depicted by the self-consistent theory. Note that ion acceleration is constant over the period for which the self-consistent equations remain valid. An experimental study by Wright et al. (1985) was conducted in a steady-state plasma flow with the density gradient created by a plate oriented perpendicular to the flow. Figure 9 provides a comparison of experimental data with the expansion front velocity predicted by the theory. It is apparent that with proper scaling of S and Φ_d, this process must be simular to the process(s) responsible for filling in the near-wake void of orbiting spacecraft; particularly in the case of large scale spacecraft.

(2) A Tethered Satellite-Electron Beam Current System

Stenzel and Urratia (1986) have investigated the current flow between a field-aligned electron beam and an electrode collecting return current on a different flux tube in a large laboratory magnetoplasma. This investigation has revealed the existence of anomalous cross-field currents

that shunt the field aligned current system, and temporal current disruptions. If these processes reflect a valid picture of large scale current systems in the earth's ionosphere, this study will be of vital importance to investigations planned with long, conducting tethered satellites (e.g., the NASA TSS-1 mission) or charged particle beam experiments on large scale structures such as the Space Station.

(3) Enhancement of Electron Temperature in the Near-Wake

An apparent electron temperature enhancement, which coincided spatially with the ion void region, was reported by Samir et al., 1974 (Figure 10). The heating of electrons may be partially explained by the effects expected to occur in the presence of a potential well, or they may result from a two-stream instability produced by an interaction between fast and slow moving ions.

5. COMPARISON OF LABORATORY AND IN SITU RESULTS

A number of laboratory experiments have allowed direct quantitative comparison with, and sometime a better understanding of, in situ measurements. Here we consider of few examples.

Several observations of an elevated electron temperature in the wake of ionospheric satellites have been reported (Samir and Wrenn, 1972; and Troy et al., 1975). This effect was investigated in the laboratory by Illiano and Storey (1974) and by Samir et al., (1974), the latter revealing electron temperature enhancements in the wake of a test body in a collisionless streaming plasma as discussed above in Section 4.2.3. The enhancement ranged up to 200 percent of the ambient stream's temperature and was confined to the void region of the plasma wake - in complete agreement withwith the in situ observations. The Samir et al. study did not establish the mechanism for electron heating in plasma wakes, but suggested it may result from a potential well in the void region or from wave particle interactions (instabilities) within the strong density gradient at the wake boundary.

Stone and Samir (1981) report on a comparison between laboratory wake experiments in which ion focusing by plasma sheath electric fields were studied (Stone, 1981b), and in situ observations of structure in the wakes of the Ariel 1 satellite and its spherical ion probe (Henderson and Samir, 1967). The laboratory results show the ion current peaks, observed at only a one axial distance in the in situ wake, to be part of an extended complex structure such as shown in Figure 3 (Stone and Samir, 1981). Moreover, the effects of body potential on the wake structure observed and quantified in the laboratory (discussed in Section 4.1.2-3) explain the similarity observed between the wakes of the satellite and the small, but negatively biased, spherical probe.

A second example presented by Stone and Samir (1981) shows that the ram/wake current ratio data, obtained from the AE-C satellite (as a function of plasma composition, electron temperature and satellite potential) can be collapsed to a single curve using the body-potential and ion acoustic Mach number dependences established in the laboratory (section 4.1.3). This example also shows that dimensionless parameters must be calculated using specific ionic mass and concentration values rather than average values.

6. INITIAL RESULTS FROM SPACE SHUTTLE MISSIONS (STS-3 AND SL-2)

By far, the most elaborate insitu investigations of spacecraft plasma electrodynamics to date have been conducted from the space shuttle. It was anticipated that the more detailed shuttle-borne experiments would complement existing in situ data and provide a sufficient data base for resolving several spacecraft-space plasma interaction issues. However the orbiter environment proved far more complex than anticipated and the main contribution to date has been a greater appreciation for the complexity of spacecraft-space plasma interactions.

The third space shuttle mission (STS-3) provided the first opportunity to measure the Orbiters plasma and field environment. This was accomplished on mission days three and four by manuevering the Plasma Diagnostic Package (PDP) up to 15 m above the Orbiter payload bay with the Remote Manipulator System (RMS) as, for example, shown in Figure 11. Differential vector measurements of ion flow direction, current density, and energy were made during this period with a Differential Ion Flux Probe (DIFP) (Stone et al., 1985). These measurements revealed the existence of secondary ion streams in the vicinity of the Orbiter at high angles of attack as great as 50° with respect to the ram direction and from 10 to 40% of the ram current intensity (see Figure 12). The source or generating mechanism for these high inclination secondary ion streams was not identified. However, their energy was close to that of the ram ions and it was concluded that they were not of geophysical origin (Stone et al., 1983).

The existence of ion streams in the disturbed plasma surrounding an orbiting body is not surprising; in fact, the existence of ion streams was inferred by Henderson and Samir (1967) and has been studied in the laboratory, as discussed in section 4.1.2. In all previous cases, the ion streams were associated with the wake region downstream from the satellite or test body and such streams were anticipated in the wake of the Orbiter. However, the secondary streams observed near the Orbiter during the STS-3 mission were totally unexpected in that they were measured when the PDP was not in the Orbiter's wake and, in some cases, when it was extended upstream from the Orbiter.

Futher analysis revealed several additional effects. Not only were high inclination ion streams typically observed, but the ion ram current direction did not, in general, correspond closely to the direction of the orbital velocity vector (see Figure 12). Moreover, in one case in which the PDP was extended above the Orbiter and oriented such that the DIFP faced directly into one of the secondary streams, the stream vanished (Stone et al., 1986). The ion current density of both the Ram and secondary streams was also found to be directly proportional to the neutral particle density as shown in Figure 13 (Stone et al., 1986).

These observations should be considered in the context of wave measurements that revealed the existence of broad band (30 H_z to 178 kH_z) electrostatic noise in the vicinity of the Orbiter (Shawhan et al., 1984) and the observation of higher than normal ambient ionospheric plasma densities (Raitt et al., 1984; Siskind et al., 1984).

The above observations, taken together, are evidence that the Orbiter travels within a neutral gas cloud that results from outgasing, thruster burns, waste dumps, etc., and that the presence of this gas cloud significantly affects the way in which the Orbiter interacts with the ambient mangetoplasma. The proportionality of the ram and secondary ion stream intensities to the density neutral particles very near the Orbiter suggest a very effective ionization mechanism. The vanishing of the secondary streams at about 10 m ahead of the Orbiter suggests that the interaction with the ionosphere may be confined within an envelope that extends on the order of 10 m in the forward direction but presumably trails out to greater distances down stream. If an electric field exists at this gas cloud-ionosphere interface, the ambient ions would be deflected such that the ramed ion current would be skewed from the Orbital velocity vector at all points except in the Orbiter's XY-plane, where the envelope would be normal, and hence the electric field parallel, to the velocity vector. This is in agreement with the trend of the data as shown in Figures 11 and 12. The motion of the secondary ion streams through the background plasma represents a large source of free energy that may be expected to generate instabilities. Recently Hwang et al. (1986) have developed a model which shows that ion streams in a background ionospheric plasma can generate electrostatic noise over the oberved spectrum.

7. CONCLUSIONS AND OPEN ISSUES

The application of laboratory plasma physics to space plasma physics and technology has proven successful in addresssing a number of issues over the past 25 years; particularly in addressing, through qualitative simulation, the overall interaction of small ionospheric satellites and instruments with the ionospheric plasma (for a review see Stone, 1981a). In the past few years, process simulation has been used to address several specific aspects of natural physical phenomenon, such as plasma expansion (Wright et al., 1986) and the bahavior of current systems in magnetosplasmas (Stenzel and Urratia, 1986). The conclusions reached in these studes have not been verified by in situ data yet and their usefulness remains to be determined - although the preliminary analysis of Spacelab 2 data suggests the existence of a process very much like the collisionless plasma expansion process studied in laboratory plasmas by Wright et al.

Through the combined efforts of laboratory and in situ investigations together with theoretical treatments, the physics of geometrically simple conducting bodies of 1 to 50 Debye lengths scale size is reasonably well understood--although certain details remain to be determined; e.g. the effects of a magnetic field on the far wake and the mechanisms producing changes in the electron distribution. This is not true, however, either for geometrically complex bodies (although previous studies (Stone, 1981a) suggest a linear superpositioning of the wakes of the simple geometric constituents, this must be more universally established), bodies with complex surface characteristics, bodies with an associated neutral gas cloud, large scale size bodies (in excess of 1,000 Debye lengths), or bodies of any type with an elevated electric potential. Future investigations of spacecraft plasma electrodynamics should therefore center around five issues; i.e.,

(1) The effects of body scale size, particularly for large scale bodies (with respect to both the Debye length and cyclotron radius).

(2) The physics of a neutral gas cloud in a hypersonic magnetoplasma.

(3) The effect of body potentials well in excess of the ionization potentials for neutral constituents.

(4) The effects of complex spacecraft geometry.

(5) The effects of complex spacecraft surface characteristics.

Moreover, these issues are of such complexity that their resolution will require laboratory investigations (that offer the advantage of comparatively low cost and fast turnaround) and theoretical treatments (that make use of recent gains in computer technology), as well as deliberate and systematic in situ experiments designed to provide data capable of corroborating the ground-based results. The previous in situ results from small ionospheric satellites were not systematic and too limited in scope, while the experiments conducted on the space shuttle involved an extremely complex body. Clearly, the required in situ experiments must be systematic, closely controlled, and use cleaner test bodies (in terms of geometric complexity, surface characteristics, gas emissions, and EMI). An understanding of the fundamental physics of hypersonic spcecraft plasma dynamics will be important to the practical application and operation of large space platforms and should not be taken lightly in planning wide usage of the space station.

REFERENCES

Astrelin, V. T., I. A. Bogashchenko, N. A. Buchel'nikova, and Yu. I. eidelman, Flow of a Magnetized Plasma Around a Plate, Soviet Phys.-Tech. Phys., 17, 1369, 1973.

Bogashchenko, I. A., A. V. Gurevich, R. A. Salimov, and Yu. I. Eidelman, Flow of Rarefied Plasma Around a Body, Soviet Phys. JETP, 32, 841, 1971.

Call, S. M., The Interaction of a Satellite with the Ionosphere, NASA CR-106555, 1969. Also Plasma Lab. Report No. 46, School of Engineering and Applied Science, Columbia University, 1969.

Chan, C., N. Hershkkowitz, A. Ferreira, T. Intrator, B. Nelson, and K. E. Lonngren, Experimental Observations of Self-Similar Plasma Expansion, Phys. Fluids, 27, 266, 1984.

Clayden, W. A. and C. V. Hurdle, An Experimental Study of Plasma-Vehicle Interaction, RGD, 2, 1717, 1966.

Falthammar, C. G., Laboratory Experiments of Magnetospheric Interest, Space Sci. Rev., 15, 803, 1974.

Fournier, G., Collisionless Plasma Flow Around a Cylinder in View of Applications to Ionospheric Probes, Publication No. 137, Office Nat. d' Etudes et de Rescherches Aerospatiales, Paris, 1971.

Fournier, G. and D. Pigache, Wakes in Collisionless Plasma, Phys. of Fluids, 18, 1443, 1975.

Gurevich, A. V., L. P. Pitaevskii, and V. V. Smirnova, Ionospheric Aerodynamics, Space Sci., Rev., 9, 805, 1969.

Hall, D. F., R. E. Kemp, and J. M. Sellen, Jr., Plasma-Vechile Interaction in a Plasma Stream, AIAA J., 2, 1032, 1964.

Henderson, C. L. and U. Samir, Observations of the Disturbed Region Around an Ionospheric Spacecraft, Planet. Space Sci., 15, 1499, 1967.

Hester, S. D. and A. A. Sonin, Some Results from a Laboratory Study of Satellite Wake Structure and Probe Response in Collisionless Plasma Flows, RGD, 2, 1659, 1969a.

Hester, S. D. and A. A. Sonin, A Laboratory Study of Electrodynamic Influences on the Wakes of Ionospheric Satellites, AIAA Paper No. 69-673 (Presented at AIAA Fluid and Plasma Dynamics Conf., San Francisco, 1969b.

Hester, S. D. and A. A. Sonin, Laboratory Study of the Wakes of Small Cylinders Under Ionospheric Satellite Conditions, Phys. Fluids, 13, 641, 1970a.

Hester, S. D. and A. A. Sonin, A Laboratory Study of the Wakes of Ionospheric Satellites, AIAA J., 8, 1090, 1970b.

Hwang, K. S., N. H. Stone, K. H. Wright, Jr., U. Samir, and D. A. Gurnett, Theoretical Investigation of Broadband Electrostatic Noise Associated with Secondary Ion Streams near the Shuttle Orbiter, MSFC Space Science Laboratory Preprint Series No. 86-113, 1986.

Illiano, J. M. and L.R.O. Storey, Apparent Enhancement of Electron Temperature in the Wake of a Spherical Probe in a Flowing Plasma, Planet. Space Sci., 22, 873, 1974.

Martin, A. R., Numerical Solutions to the Problem of Charged Particle Flow Around an Ionospheric Spacecraft, Planet. Space Sci., 22, 121, 1974.

Maslennikov, M. V. and Yu S. Sigov, A Discrete Model for the Study of the Flow of a Rarefied Plasma About a Body, Soviet Phys. Doklady, 9, 1063, 1965.

Maslennikov, M. V. and Yu. S. Sigov, Discrete Model of Medium in a Problem on Rarefied Plasma Stream Interaction with a Charged Body, RGD, 2, 1657, 1967.

Maslennikov, M. V., Yu. S. Sigov, and G. P. Charkina, Numerical Experiments on Flow of a Rarefied Plasma Around Bodies of Various Shapes, Cosmic Res., 6, 184, 1968.

Maslennikov, M. V. and Yu. S. Sigov, Rarefied Plasma Stream Interactions with Charged Bodies of Various Forms, RGD, 2, 1671, 1969.

Raitt, W. J., D. E. Siskind, P. M. Banks, and P. R. Williamson, Measurements of the Thermal Plasma Environment of the Space Shutle, Planet. Space Sci., 32, 457, 1984.

Rand, S., Wake of a Satellite Traversing the Ionosphere, Phys. Fluids, 3, 265, 1960a.

Rand, S., Dampening of the Satellite Wake in the Ionosphere, Phys. Fluids, 3, 588, 1960b.

Samir, U. and G. L. Wrenn, Experimental Evidence of an Electron Temperature Enhancement in the Wake of an Ionospheric Satellite, Planet. Space Sci., 20, 899, 1972.

Samir, U., Charged Particle Distribution in the Nearest Vicinity of Ionospheric Satellites - Comparison of the Main Results from the Ariel I, Explorer 31 and Gemini-Agena 10 Spacecraft. Photon and Particle Interations with Surfaces in Space, (R.J.L. Grard, Ed.) pp. 193-219, D. Reidel Pub. Co., Dordrecht, Holland, 1973.

Samir, U., W. A. Oran, and N. H. Stone, Laboratory Simulation of Space Aerodynamic Phenomena, Satellite Wake Studies, Rarefied Gas Dyn., Proc. Int. Symp. 9th, 2, D11.1, 1974a.

Samir, U., N. H. Stone, and W. A. Oran, Does a "Two-Stream" Flow Model Apply to Wakes of Large Bodies in Space? Astrophys and Space Sci., 31, L1, 1974b.

Samir, U, K. H. Wright, Jr., and N. H. Stone, The Expansion of a Plasma into a Vacuum: Basic Phenomena and Processes and Applicationa to Space Plasma Physics, J. Geophys. Res., 21, 1631, 1983.

Shawhan, S. D., G. B. Murphy, and J. S. Pickett, Plasma Diagnostics Package Initial Assessment of the Orbiter Plasma Environment, J. Spacecr. Rockets, 21, 387, 1984.

Siskind, D. E., W. J. Raitt, P. M. Banks, and P. R. Williamson, Interactions Between the Orbiting Space Shuttle and the Ionosphere, Planet. Space Sci., 32, 881, 1984.

Skvortsov, V. V. and L. V. Nosachev, The Structure of the Trail Behind a Spherical Model in a Stream of Rarefied Plasma, Cosmic Res., 6, 191, 1968b.

Skvortsov, V. V. and L. V. Nosachev, Some Results on Disturbances Introduced by Extraneous Bodies into a Stream of Rarefied Plasma, Cosmic Res., 6, 718, 1968b.

Stenzel, R. L. and J. M. Urrutia, Laboratory Model of a Tethered Balloon - Electron Beam Current System, Geophys. Res. Lett., 13, 797, 1986.

Stone, N. H., W. A. Oran, and U. Samir, Collisionless Plasma Flow Over a Conducting Sphere, Planet. Space Sci., 20, 1787, 1972.

Stone, N. H., U. Samir, and W. A. Oran, Laboratory Simulation of the Structure of Disturbed Zones Around Bodies in Space, JATP, 36, 253, 1974.

Stone, N. H., U. Samir, and K. H. Wright, Jr., Plasma Disturbances Created by Probes in the Ionosphere and Their Potential Impact on Low-Energy Measurements Considered for Spacelab, JGR, 83, 1668, 1978.

Stone, N. H., The Aerodynamics of Bodies in a Rarefied Ionized Gas with Applications to Spacecraft Environmental Dynamics, NASA TP 1933, 1981a.

Stone, N. H., The Plasma Wake of Mesosonic Conducting Bodies, Part 1, An Experimental Parametric Study of Ion Focusing by the Plasma Sheath, J. Plasma Phys., 25, 351, 1981b.

Stone, N. H., The Plasma Wake of Mesosonic Conducting Bodies, Part 2, An Experimental Parametric Study of the Mid-Wake Ion Density Peak, J. Plasma Phys., 26, 386, 1981c.

Stone, N. H. and U. Samir, Bodies in Flowing Plasmas, Laboratory Studies, Adv. Space Res., 1, 361, 1981.

Stone, N. H. U. Samir, K. H. Wright, Jr., D. L. Reasoner, and S. D. Shawhan, Multiple Ion Streams in the Near Vicinity of the Space Shuttle, Geophys. Res. Lett., 10, 1215, 1983.

Stone, N. H., J. J. Lewter, W. H. Chisholm, and K. H. Wright, Jr., Instrument for Differential Ion Flux Vector Measurements on Spacelab 2, Rev. Sci. Instrum., 56, 1897, 1985.

Stone, N. H., K. H. Wright, Jr. K. S. Hwang, U. Samir, G. B. Murphy, and S. D. Shawhan, Further Observations of Space Shuttle Plasma-Electrodynamic Effects from OS31/STSJ-3, Geophys. Res. Lett., 13, 217, 1986.

Taylor, J. C., Disturbance of a Rarefied Plasma by a Supersonic Body on the Basis of the Poisson-Vlasov Equations - I and II, Planetary Space Sci., 15, 155 and 463, 1967.

Troy, Jr., B. E. E. J. Maier, and U. Samir, Electron Temperatures in the Wake of an Ionospheric Satellite, JGR, 80, 993, 1975.

Woodroffe, J. A., and A. A. Sonin, Calculation for the Wake of a Small Cylinder Under Ionospheric Satellite Conditions, Phys. Fluids, 17, 79, 1974.

Wright, K. H. N. H. Stone, and U. Samir, A Study of Plasma Expansion Phenomena in Laboratory Generated Plasma Wakes: Preliminary Results, J. Plas. Phys., 33, 71, 1985.

Wright, K. H., D. E. Parks, I. Katz, N. H. Stone, and U. Samir, More on the Expansion of a Collisionless Plasma into the Wake of a Body, J. Plas. Phys., 35, 119, 1986.

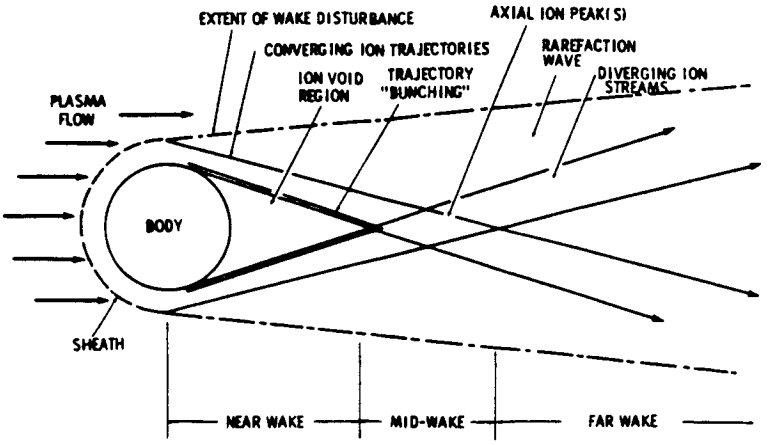

Figure 1. Ion behavior within disturbed zone. After Stone [1981a].

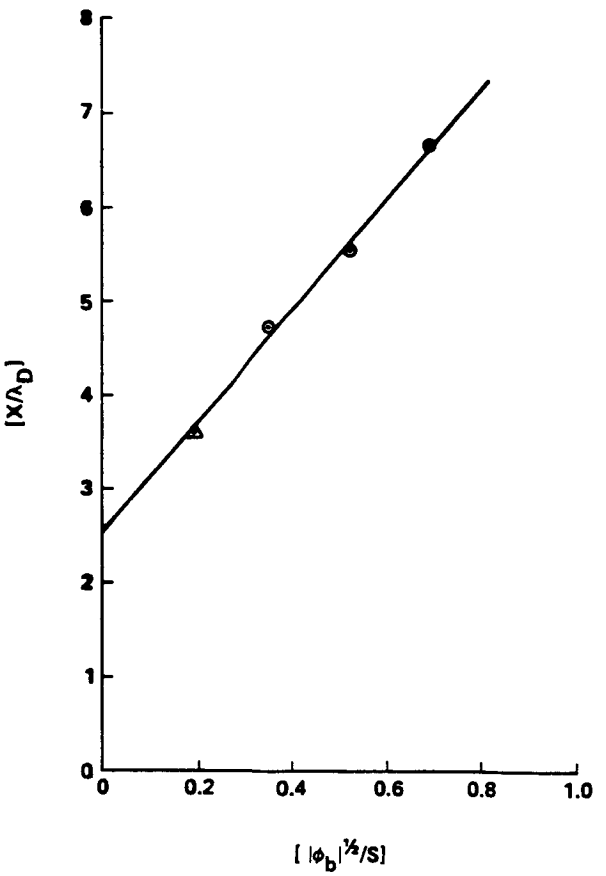

Figure 2. Dependence of the sheath width at the critical cross-section of a test body (x/λ_D) on body potential and ion acoustic Mach number. Open circles represent data for a sphere and open triangles for a parallel cylinder. After Stone et al. [1978].

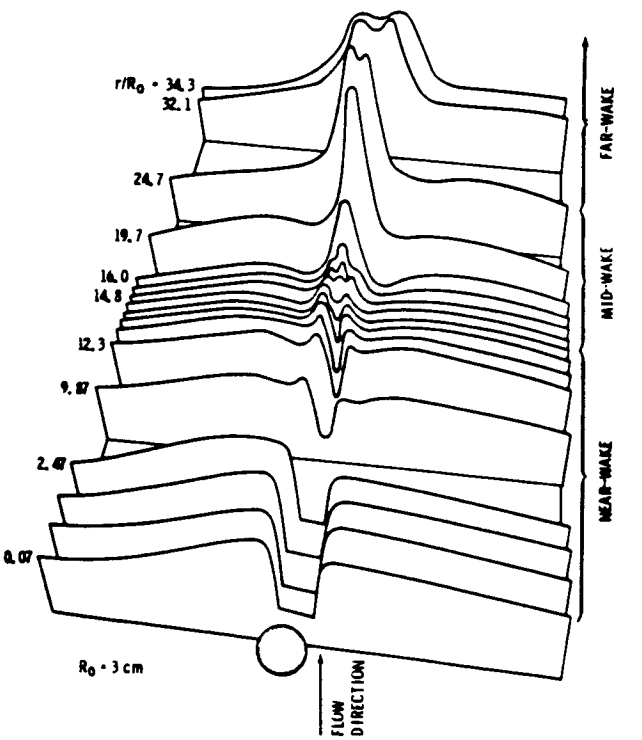

Figure 3. Ion current density profiles downstream from a conducting sphere (R_o = 3 cm) for $R_d \tilde{=} 0.8$, S ≈ 17, and $\phi_b \approx -5$, data after Stone et al. [1972].

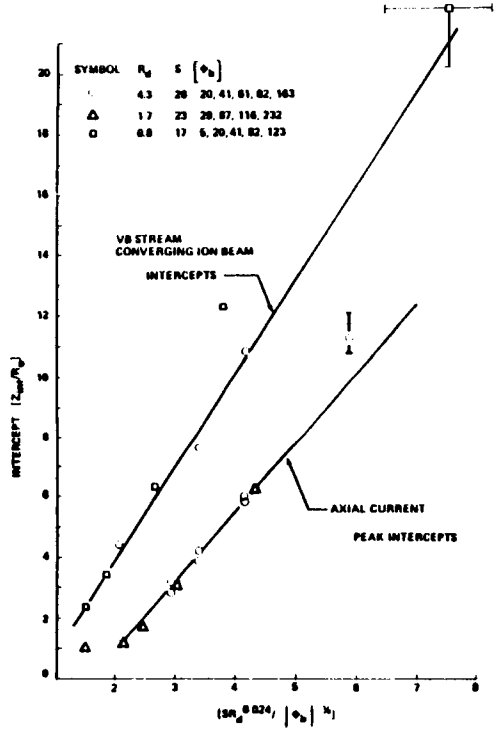

Figure 4. Variation of axial ion peak intercepts and the crossing point for converging ion streams with $\left[S\ R_o^{\alpha}/|\phi_b|^{1/2}\right]$. After Stone [1981c].

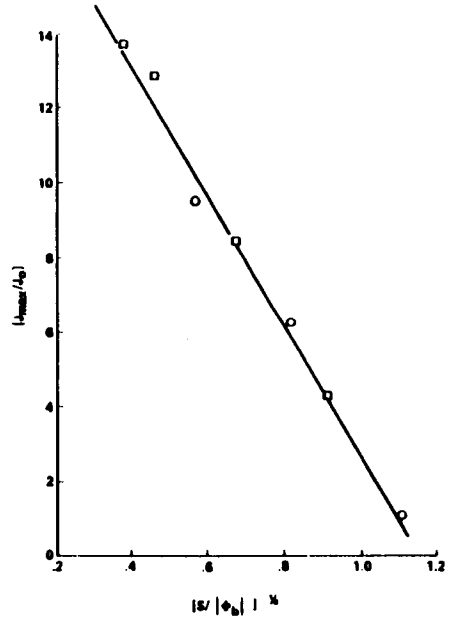

Figure 5. Variation of the normalized maximum amplitude of the axial ion peak, $[J_{max}/J_o]$ with $\left[S/|\phi_b|\right]^{1/2}$. After Stone [1981c].

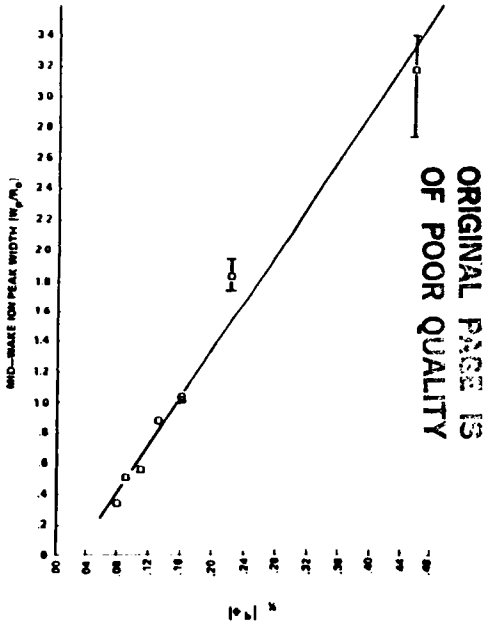

Figure 6. Variation of the axial ion peak width at half maximum with $|\phi_b|^{-1/2}$. After Stone [1981c].

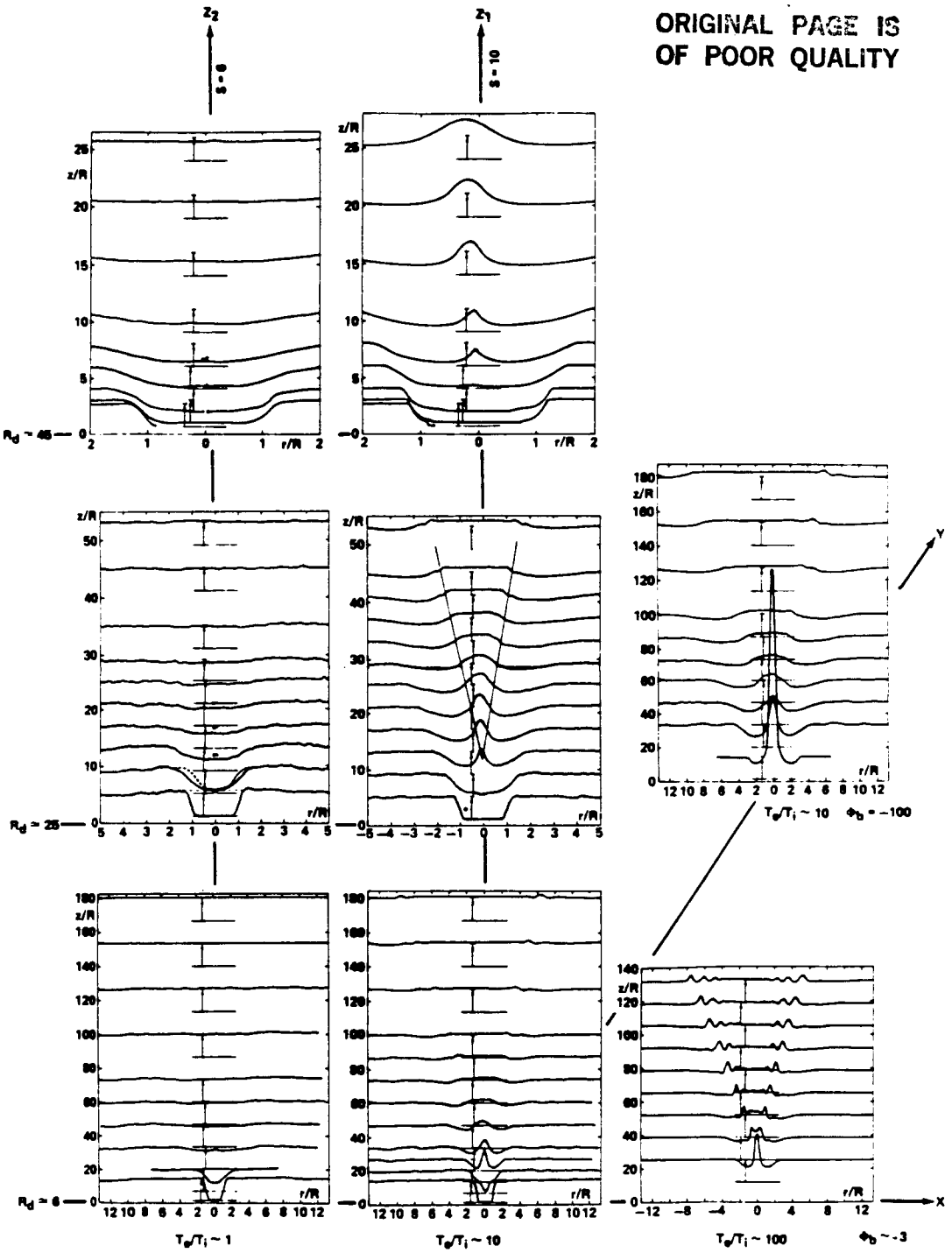

Figure 7. The ion current density in the wakes of spherical test bodies for the conditions, $P \tilde{=} 1.6 \times 10^{-7}$ torr, $S \sim 10$ (except under the Z_2 -axis where $S \tilde{=} 6$), $E_i = 20$ eV, $T_{eo} = 1400$ to $2000°K$, X-axis = $f(T_e/T_i)$, Y-axis = $f(\Phi_b)$ and Z-axis = $f(R_d)$. After Fournier and Pigache [1975].

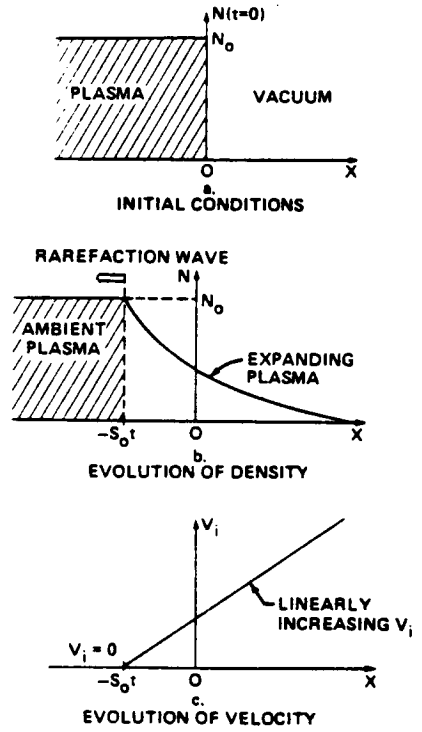

Figure 8. Schematic of plasma expansion into a vacuum. (a) Initial condition, (b) Evolution of density, (c) Evolution of ion velocity according to the self-similar treatment. After Samir et al. [1983].

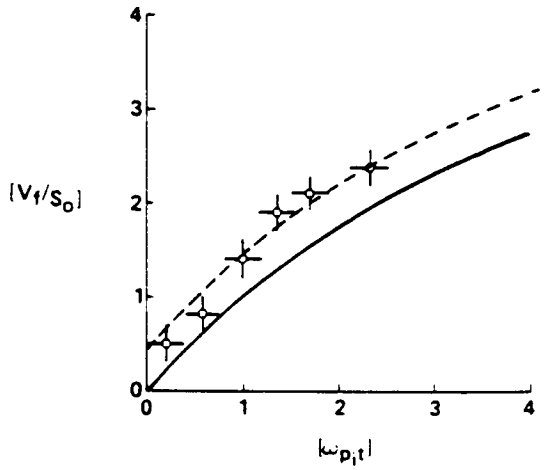

Figure 9. Ion velocity at the expansion front vs time. O, laboratory measurements, --, theoretical model. After Wright et al. [1986].

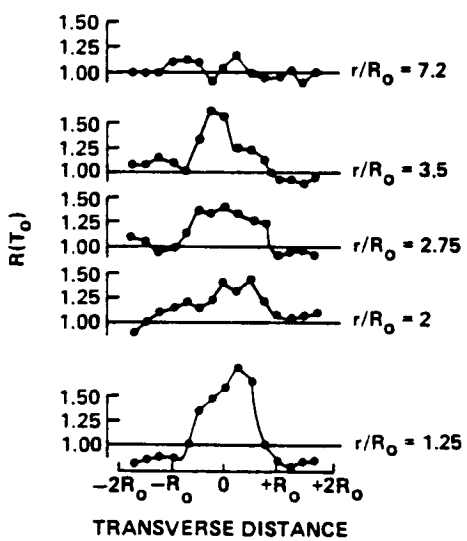

Figure 10. Transverse profiles of $[T_e\ (\text{wake})/T_{eo}]$ downstream from a conducting sphere for T_e = 1200 K°, count n = 7.5 x $10^4/cm^3$, E_i = 5.3 eV. After Samir et al. [1974].

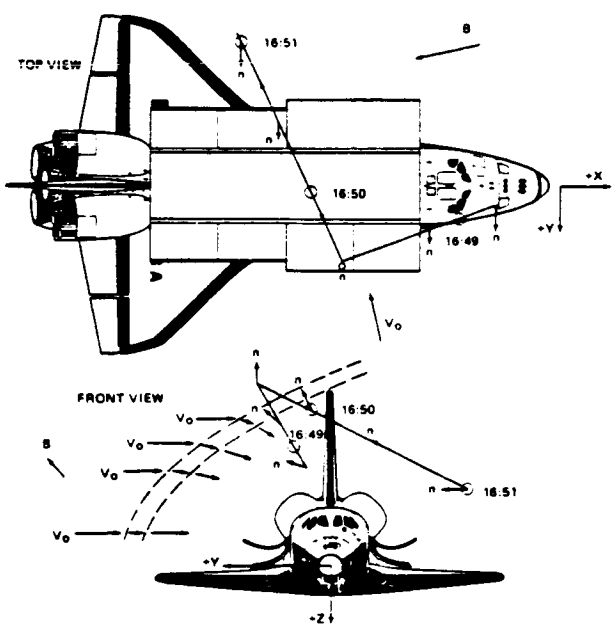

Figure 11. PDP track on Julian day 85 for the period 16:48:40 to 16:51:05. DIFP normal is indicated by n. Dashed lines indicate the inferred boundary of the interaction region. After Stone et al. [1986].

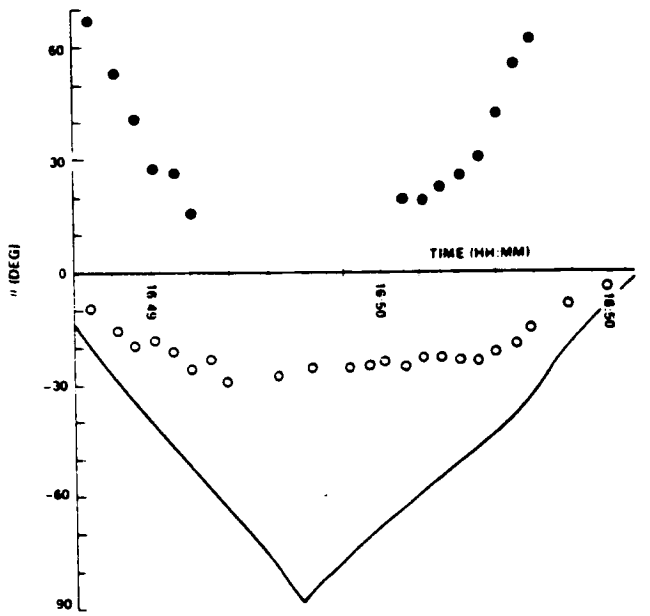

Figure 12. Angles-of-attack of the ram ion current (open circles) and secondary ion steam (closed circles) for the period indicated in Fig. 11. Solid line is the angle between the DIFP normal and the orbital velocity vector. After Stone et al. [1986].

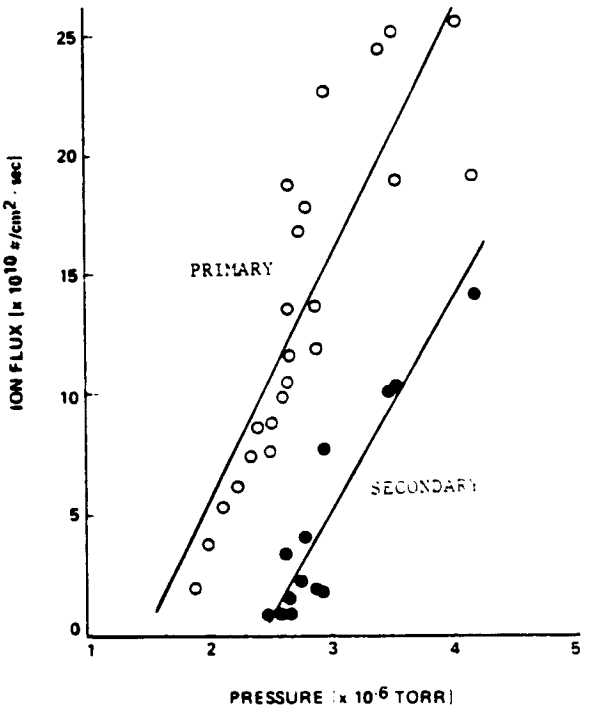

Figure 13. Ion current density vs pressure (neutral particle density) for the period indicated in Fig. 11. After Stone et al. [1986].